The EMBO Journal (2010) 29, 2070–2081 | © 2010 European Molecular Biology Organization | All Rights Reserved 0261-4189/10
www.embojournal.org

THE EMBO JOURNAL

CaMKIIα interacts with M4 muscarinic receptors to control receptor and psychomotor function

Ming-Lei Guo[1], Eugene E Fibuch[2], Xian-Yu Liu[3], Eun Sang Choe[4], Shilpa Buch[5], Li-Min Mao[1,*] and John Q Wang[1,2,*]

[1]Department of Basic Medical Science, University of Missouri-Kansas City, Kansas City, MO, USA, [2]Department of Anesthesiology, School of Medicine, University of Missouri-Kansas City, Kansas City, MO, USA, [3]Department of Anesthesiology, Washington University School of Medicine, St Louis, MO, USA, [4]Department of Biological Sciences, Pusan National University, Kumjeong-gu, Pusan, Korea and [5]Department of Pharmacology and Experimental Neuroscience, University of Nebraska Medical Center, Omaha, NE, USA

Muscarinic acetylcholine receptors (mAChRs) are widely expressed in the mammalian brain and are essential for neuronal functions. These receptors are believed to be actively regulated by intracellular signals, although the underlying mechanisms are largely unknown. In this study, we show that Ca^{2+}/calmodulin-dependent protein kinase II (CaMKII) binds directly and selectively to one of five mAChR subtypes, M4 receptors (M4Rs), at their C-terminal regions of second intracellular loops. This binding relies on Ca^{2+} activation of the kinase and leads to the phosphorylation of M4Rs at a specific threonine site (Thr145). Complementary *in vivo* studies in rat striatal neurons enriched with M4Rs confirm that rising Ca^{2+} recruits CaMKIIα to M4Rs to potentiate receptor signalling, which controls behavioural sensitivity to dopamine stimulation in an activity-dependent manner. Our data identify a new model of protein–protein interactions. In a Ca^{2+}-sensitive manner, CaMKIIα regulates M4R efficacy and controls the acetylcholine–dopamine balance in the basal ganglia and also the dynamics of movement.

The EMBO Journal (2010) **29,** 2070–2081. doi:10.1038/emboj.2010.93; Published online 11 May 2010
Subject Categories: signal transduction; neuroscience
Keywords: calcium; cAMP; cocaine; phosphorylation; striatum

Introduction

Muscarinic acetylcholine receptors (mAChRs) are widely expressed in neurons, cardiac and smooth muscles, and many other tissues (Nathanson, 2008). As members of the G protein-coupled receptor (GPCR) superfamily, five muscarinic receptor subtypes (M1–M5) are subdivided into two functional groups (Wess, 1996; Nathanson, 2000). In general, the M1, M3, and M5 subtypes are preferentially coupled to Gαq proteins. As such, they activate phospholipase C to trigger a phosphoinositide-dependent signalling pathway. The M2 and M4 subtypes, however, are coupled to Gαi/o proteins. Through them, they inhibit adenylyl cyclase and the downstream formation of cAMP. The broad expression and diverse signalling pathway connections enable mAChRs to regulate various cellular activities. In rodent brains, mAChRs are enriched in the striatum (Nathanson, 2008). Particularly, M4 receptors (M4Rs) are most abundantly present in this region and are preferentially localized at post-synaptic sites (Levey *et al*, 1991; Yasuda *et al*, 1993; Hersch *et al*, 1994). This situates M4Rs well to regulate striatal cellular activity related to learning, memory, cognition, reward, and movement. Moreover, malfunctional M4Rs are frequently linked to the pathogenesis of mental illnesses, such as schizophrenia and substance addiction, and neurodegenerative disorders, such as Parkinson's and Alzheimer's diseases (Langmead *et al*, 2008; Scarr and Dean, 2008).

The G protein-coupled receptors are actively regulated by protein–protein interactions between their intracellular domains and submembranous regulatory proteins. Among all regulatory proteins, protein kinases are of particular importance. Various serine/threonine protein kinases can directly or indirectly interact with GPCRs. Through a phosphorylation mechanism, they drastically modulate the efficacy of receptor signalling. Ca^{2+}/calmodulin-dependent protein kinase II (CaMKII) is among those kinases that regulate GPCR signalling via a mechanism involving interaction and phosphorylation. This enzyme is especially abundant in brain cells and is enriched at synaptic sites (Kelly *et al*, 1984). It is activated by the binding of Ca^{2+} and calmodulin (CaM). Activated CaMKII can then access and phosphorylate both exogenous substrates and its own autophosphorylation site (T286 in the α isoform). Such autophosphorylation renders the enzyme a Ca^{2+}/CaM-independent (autonomous) activity even after the initial Ca^{2+} stimulus subsides (Hudmon and Schulman, 2002; Colbran and Brown, 2004; Griffith, 2004). As a result, CaMKII can transmit a transient Ca^{2+} signal into the relatively prolonged regulation of its downstream targets (for review, see Hudmon and Schulman, 2002; Lisman *et al*, 2002; Colbran and Brown, 2004).

Although CaMKII is believed to interact with and regulate many targets (Colbran, 2004), a limited number of such interacting partners have been identified. In this study, we identify that CaMKIIα interacts directly with the C-terminal region of the second intracellular loop of M4Rs *in vitro*. The interaction is dependent on Ca^{2+} level and autophosphorylation. The inducible interaction enables CaMKIIα to phosphorylate M4Rs at a selective threonine residue within the binding motif. In striatal neurons *in vivo*, Ca^{2+} stimulates the association of CaMKIIα with M4Rs and increases threonine phosphorylation of M4Rs, which thereby potentiates M4R efficacy. The CaMKII-mediated potentiation of M4Rs has a significant role in regulating behavioural responsiveness to dopamine

*Corresponding authors. JQ Wang or L-M Mao, Department of Basic Medical Science, University of Missouri-Kansas City, School of Medicine, 2411 Holmes Street, Kansas City, MO 64108, USA.
Tel: +1 816 235 1786; Fax: +1 816 235 5574;
E-mail: wangjq@umkc.edu or Tel: +1 816 235 1719;
Fax: +1 816 235 5574; E-mail: maol@umkc.edu

Received: 11 January 2010; accepted: 20 April 2010; published online: 11 May 2010

stimulation with cocaine. Together, our data reveal a new model of protein–protein interactions. Through this interaction, CaMKII participates in maintaining a proper acetylcholine–dopamine balance in the striatum.

Results

CaMKIIα selectively binds to M4Rs

Rat M4Rs possess four intracellular domains: three intracellular loops and one C-terminus (Supplementary Figure S1). To explore whether cytoplasmic CaMKIIα interacts with any of these domains, we synthesized a panel of glutathione-*S*-transferase (GST) fusion proteins containing full, or fragments of, individual domains (Figure 1A). Using these GST-immobilized baits in pull-down assays with rat soluble striatal lysates, we observed that the GST-tagged second intracellular loop of M4Rs (GST–M4R$_{IL2}$) pulled down CaMKIIα (Figure 1B), whereas ther GST fusion proteins and GST alone did not. The GST fusion protein containing the second intracellular loop of muscarinic M2 receptors (M2Rs)

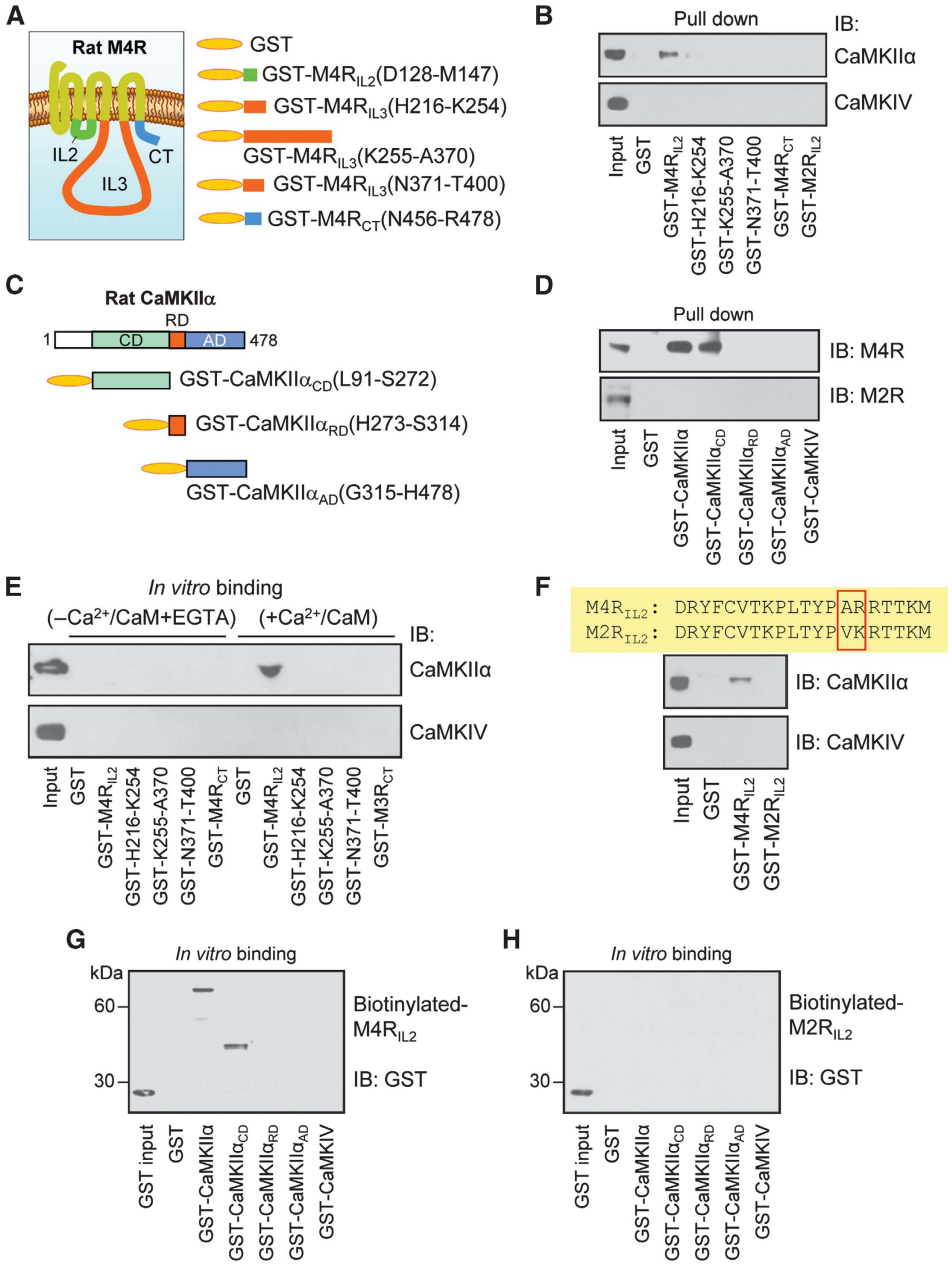

Figure 1 Interactions of CaMKIIα with M4Rs. (**A**) GST fusion proteins containing the second intracellular loop (IL2), third intracellular loop (IL3) fragments, and C-terminus (CT) of rat M4Rs. (**B**) Pull-down assays with immobilized GST fusion proteins and rat striatal lysates. (**C**) GST fusion proteins derived from rat CaMKIIα. (**D**) Pull-down assays showing that GST–CaMKIIα and GST–CaMKIIα$_{CD}$ pulled down M4Rs from rat striatal lysates. (**E**, **F**) *In vitro* binding assays with immobilized GST fusion proteins and purified CaMKIIα or CaMKIV. (**G**, **H**) *In vitro* binding assays with immobilized biotinylated-M4R$_{IL2}$ or -M2R$_{IL2}$ and purified GST–CaMKIIα fragments or GST–CaMKIV. Binding assays in (**E**) were performed in the presence or absence of $CaCl_2$ (0.5 mM), CaM (1 μM), or EGTA (1 mM). Other binding assays (**F**–**H**) were conducted in the presence of $CaCl_2$ (0.5 mM) and CaM (1 μM). Proteins bound to GST fusion proteins (**B**, **D**–**F**) or biotinylated proteins (**G**, **H**) in either pull-down or binding assays were visualized with immunoblots (IBs) using the specific antibodies as indicated.

also did not pull down CaMIIα. None of the GST fusion proteins pulled down CaMKIV, another isoform of CaMK. Blots that were probed in parallel with an anti-GST antibody ensured equivalent protein loading (Supplementary Figure S2A). To identify the region within CaMKIIα involved in the interaction with M4Rs, we prepared GST fusion proteins containing each key structure of the kinase (Figure 1C). We observed that the N-terminal catalytic domain of CaMKIIα (GST–CaMKIIα$_{CD}$), similar to the full-length GST–CaMKIIα, precipitated M4Rs in pull-down experiments with striatal lysates (Figure 1D). The GST fusion proteins containing the regulatory domain (GST–CaMKIIα$_{RD}$) or the C-terminal association domain (GST–CaMKIIα$_{AD}$) produced no precipitation. We did not observe that GST–CaMKIV pulled down M4Rs. Furthermore, none of the GST fusion proteins pulled down M2Rs (Figure 1D). Thus, a restricted region of the enzyme, that is, CaMKIIα$_{CD}$, is responsible for the M4R interaction.

We next examined whether CaMKIIα directly interacts with M4Rs in binding assays with purified proteins. CaMKIIα rather than CaMKIV bound to immobilized GST–M4R$_{IL2}$, but not to other GST–M4R$_{IL3}$ fragments, GST–M4R$_{CT}$, or GST alone (Figure 1E). Interestingly, CaMKIIα exhibited the binding only in the presence of Ca^{2+}/CaM. In the absence of Ca^{2+}/CaM, wherein the enzyme remains inactive, no binding was detected. Thus, activation of the enzyme by Ca^{2+}/CaM is required for its binding. CaMKIIα also bound to full-length M4Rs (Supplementary Figure S2B). However, CaMKIIα did not bind to GST–M2R$_{IL2}$ (Figure 1F). This is noteworthy given that only two residues are different between M2R$_{IL2}$ and M4R$_{IL2}$ (Figure 1F). Further assays aimed at screening the binding of CaMKIIα to the second intracellular loops of all five muscarinic subtypes revealed that the kinase bound only to M4R$_{IL2}$ (Supplementary Figure S2C), a domain highly conserved among mammals (Supplementary Figure S2D). We also tried to immobilize biotinylated M4R$_{IL2}$ and subsequently tested the binding of GST fusion CaMKIIα fragments to M4R$_{IL2}$. The bound GST fusion proteins were visualized by immunoblots with an anti-GST antibody. We observed that the immobilized M4R$_{IL2}$ was bound by GST–CaMKIIα and GST–CaMKIIα$_{CD}$, but not by other GST–CaMKIIα fragments or GST–CaMKIV (Figure 1G). The immobilized M2R$_{IL2}$ was not bound by any GST fusion proteins (Figure 1H). These results indicate that CaMKIIα and M4Rs bind directly to each other through their defined subdomains.

Ca^{2+} and autophosphorylation regulate CaMKIIα binding to M4R$_{IL2}$

The Ca^{2+}-dependent nature of CaMKIIα–M4R binding was further investigated. Similar to the results described above, the addition of Ca^{2+} (0.5 mM) and CaM (1 μM) enabled CaMKIIα to bind to M4R$_{IL2}$ (L2 versus L1 in Figure 2A). In contrast, the Ca^{2+}/CaM binding-defective CaMKIIα mutant, T305/306D (Colbran and Soderling, 1990), showed no binding regardless of the presence of Ca^{2+}/CaM (Figure 2A). Adding a peptide (L290–A309), which corresponds to the CaM-binding domain of CaMKII and thereby antagonizes the CaM–CaMKII association, blocked the Ca^{2+}/CaM-induced binding between CaMKIIα and M4Rs (Figure 2B). Similar effect was observed with a Ca^{2+} chelator EGTA (1 mM; data not shown). These results substantiate the model that activation of CaMKIIα by Ca^{2+}/CaM is essential to transform the kinase to a state preferred for physical interaction with M4Rs. Notably, CaMKIIα can bind to M4Rs in a form bearing no autophosphorylation at T286. This was evidenced by the lack of detectable T286-autophosphorylated CaMKIIα (pCaMKIIα) in the binding assays containing no ATP (a preferred phosphate donor) (middle panel of Figure 2A). Thus, activation of CaMKIIα by Ca^{2+}/CaM is sufficient to promote the binding of the enzyme to M4Rs.

The autophosphorylation of T286 may further impact on binding properties of the kinase. To examine this, we tested the binding capacity of autophosphorylated CaMKIIα. We found that CaMKIIα that was activated by Ca^{2+}/CaM and autophosphorylated at T286 before the binding assays exhibited a higher level of binding to GST–M4R$_{IL2}$ compared with unphosphorylated CaMKIIα (L4 versus L2 in Figure 2C and E). In the absence of Ca^{2+}/CaM in binding reactions, autophosphorylated rather than unphosphorylated CaMKIIα bound to the target (L3 versus L1 in Figure 2C). These data indicate that the autophosphorylation further enhances the binding and that, once autophosphorylated, the kinase no longer relies on Ca^{2+}/CaM to bind to M4Rs. In support of this, an autophosphorylation-defective mutant, T286A, showed no further enhancement of the binding (L4 versus L2 in Figure 2D and E). A constitutively active mutant, T286D, that has the same property as autophosphorylated CaMKIIα, showed a high level of binding, regardless of the presence or absence of Ca^{2+}/CaM (Figure 2D and E).

To identify a core binding motif within the 20 amino acids of M4R$_{IL2}$, we used a panel of peptides truncated from M4R$_{IL2}$ to compete with full-length M4R$_{IL2}$ for binding to CaMKIIα. Four peptides (a–d) completely prevented GST–M4R$_{IL2}$ from precipitating Ca^{2+}/CaM-activated CaMKIIα (Figure 2F) or autophosphorylated CaMKIIα (Supplementary Figure S3). These findings seem to suggest a 9-residue sequence (YPARRTTKM) as a core binding motif for CaMKIIα.

Phosphorylation of M4R$_{IL2}$ by CaMKII

The biochemical binding of CaMKIIα to M4R$_{IL2}$ suggests the latter to be a potential phosphorylation substrate of the kinase. To determine this, we assayed the CaMKIIα-mediated incorporation of ^{32}P into M4R$_{IL2}$ by sensitive autoradiography. We observed that activated CaMKIIα in the presence of Ca^{2+}/CaM phosphorylated GST–M4R$_{IL2}$ but not GST, whereas the inactive CaMKIIα in the absence of Ca^{2+}/CaM did not (Figure 3A). In separate assays, active CaMKIIα did not phosphorylate three GST–M4R$_{IL3}$ fragments and GST–M4R$_{CT}$ (Figure 3B). Consistent with the fact that CaMKIIα did not bind to M2R$_{IL2}$, the kinase induced little or no phosphorylation of GST–M2R$_{IL2}$ (Figure 3C). In fact, among all the five muscarinic receptor subtypes, CaMKIIα induced a strong phosphorylation only in M4R$_{IL2}$ (Supplementary Figure S4). These data identify M4R$_{IL2}$ as a preferred substrate for selective phosphorylation by CaMKIIα. To identify accurate phosphorylation site(s) within M4R$_{IL2}$, we screened phosphorylation of a series of synthetic M4R$_{IL2}$ peptides bearing mutations of four known threonine sites (Figure 3D). CaMKIIα readily phosphorylated a wild-type (WT) M4R$_{IL2}$ peptide substrate to a substantial stoichiometry (0.62 mol of phosphate per mol of substrate, Figure 3D). The kinase also phosphorylated the peptide with mutation of T134 to alanine (T134A), T138 to alanine (T138A), or T144 to alanine (T144A) to an extent comparable with the WT peptide. Remarkably, mutation of T145 to alanine (T145A) completely

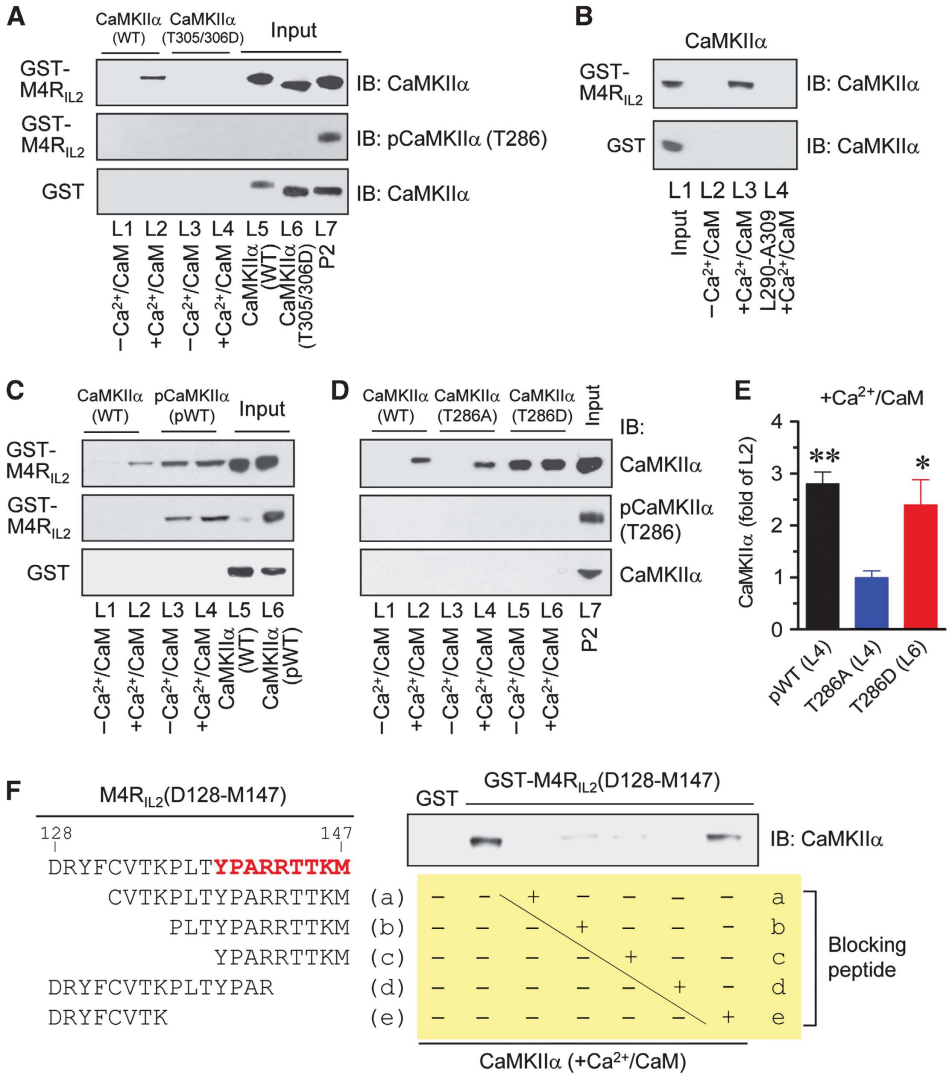

Figure 2 Ca^{2+}/CaM- and autophosphorylation-regulated CaMKIIα binding to M4R$_{IL2}$. (**A**) CaMKIIα T305/306D mutant lacks the binding to M4R$_{IL2}$. In the middle panel, CaMKIIα was not autophosphorylated at T286 in binding assays lacking ATP (L1–L4) as opposed to T286-autophosphorylated CaMKIIα detected in the synaptosomal fraction (P2) from the rat striatum (L7) with a phospho-specific antibody. (**B**) The inhibitory peptide (L290–A309) prevented the Ca^{2+}/CaM-induced CaMKIIα-M4R$_{IL2}$ binding. (**C**, **D**) Binding of WT CaMKIIα/pCaMKIIα (**C**), mutant T286A (**D**), or mutant T286D (**D**) to GST–M4R$_{IL2}$. (**E**) A graph of the data from (**C**, **D**). (**F**) Effects of five peptides derived from M4R$_{IL2}$ on the binding of CaMKIIα to M4R$_{IL2}$. Bold letters (in red) indicate the potential CaMKIIα-binding motif. Binding assays were performed between His-tagged WT CaMKIIα (~57 kDa), WT pCaMKIIα (~57 kDa), T305/306D mutant (~50 kDa), T286A mutant (~50 kDa), or T286D mutant (~50 kDa) proteins and immobilized GST or GST–M4R$_{IL2}$ in the presence or absence of $CaCl_2$ (0.5 mM), CaM (1 μM), or L290–A309 (5 μM) as indicated. EGTA (1 mM) was added in the assays lacking $CaCl_2$. Bound CaMKIIα, pCaMKIIα, or mutants were visualized by immunoblots. Data are presented as means ± s.e.m. for 4–6 experiments per group. $^*P<0.05$ and $^{**}P<0.01$ versus L2.

abolished the phosphorylation. So did mutation of all four threonine sites to alanine. These data support T145 to be the site of phosphorylation within M4R$_{IL2}$. Notably, the CaMKIIα-mediated phosphorylation at this site is comparable with that at a threonine site in a classical CaMKII substrate, autocamtide-2 (KKALRRQETVDAL, Figure 3E). To determine whether this Ca^{2+}-dependent phosphorylation was physiologically relevant, we tested the phosphorylation of M4R$_{IL2}$ at physiological Ca^{2+} concentrations. At two physiological concentrations, CaMKIIα reliably phosphorylated M4R$_{IL2}$ (Figure 3F), but not M2R$_{IL2}$ (Figure 3G).

In vivo interactions of CaMKIIα with M4Rs

We next wanted to define whether the protein–protein interaction between native CaMKIIα and M4Rs occurs in neurons *in vivo*. We targeted the striatum because it exhibits the highest level of M4Rs in the brain (Levey *et al*, 1991; Yasuda *et al*, 1993; Hersch *et al*, 1994). In addition, M4Rs are a predominant subtype in this region as they account for 45% of total mAChRs, whereas M1Rs and M2Rs account for 35 and 12%, respectively. To assess the interaction, we performed a series of co-immunoprecipitation experiments with the solubilized synaptosomal fraction (P2) from the rat striatum. We observed that a CaMKIIα-immunoreactive band was consistently seen in the proteins precipitated by an anti-M4R antibody (Figure 4A). No immunoreactivity of CaMKIV was detected in the M4R precipitates. In reverse co-immunoprecipitation assays, an M4R-immunoreactive band was displayed in the CaMKIIα precipitates, whereas the M2R immunoreactivity was not (Figure 4B). These data demonstrate an evident interaction between CaMKIIα and M4Rs in striatal neurons *in vivo*. This interaction and its specificity were

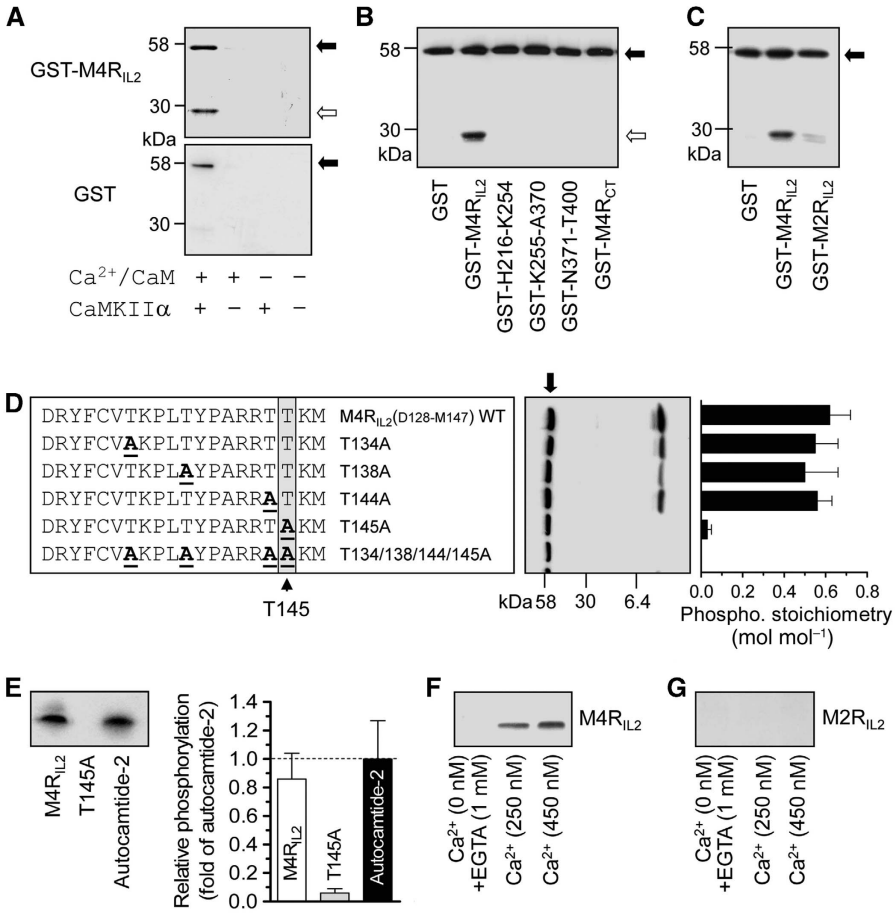

Figure 3 Phosphorylation of M4R$_{IL2}$ by CaMKIIα. (**A**) Autoradiographs illustrating phosphorylation of GST–M4R$_{IL2}$ (upper) but not GST (lower) in the presence of Ca^{2+}/CaM. (**B**) An autoradiograph illustrating phosphorylation of GST–M4R$_{IL2}$ but not other GST fusion proteins. (**C**) An autoradiograph illustrating phosphorylation of GST–M4R$_{IL2}$ but not GST–M2R$_{IL2}$. (**D**) Phosphorylation of synthetic peptides (WT or mutants). An autoradiograph shows phosphorylation of these peptides. Phosphorylation stoichiometry was calculated from the radioactivity measured on Coomassie-stained bands by liquid scintillation counting. (**E**) Phosphorylation of M4R$_{IL2}$ and autocamtide-2. ^{32}P densitometry of two phosphorylated peptides (2 μM) was directly quantified on the films. (**F**, **G**) Phosphorylation of M4R$_{IL2}$ but not M2R$_{IL2}$ at physiological concentrations of Ca^{2+}. Phosphorylation reactions were carried out at 30°C for 10 min with [γ-^{32}P]ATP in the presence of Ca^{2+} (0.5 mM)/CaM (1 μM) or as indicated. The reactions were then subjected to gel electrophoresis followed by autoradiograph. The solid arrows indicate autophosphorylated CaMKIIα, whereas open arrows indicate phosphorylated GST–M4R$_{IL2}$. Data are presented as means ± s.e.m. for 3–5 experiments per group.

further confirmed by experiments in mutant mice. In M4R-deficient mice, co-immunoprecipitation of the two proteins was not seen in the striatum, whereas it was evident in the WT mice (Figure 4C).

Ca^{2+} regulates CaMKIIα–M4R interactions in vivo

To determine whether Ca^{2+} regulates CaMKIIα–M4R interactions *in vivo* as seen *in vitro*, we subjected rat striatal slices to a Ca^{2+} ionophore, ionomycin. We then assayed changes in interaction levels of two proteins using co-immunoprecipitation. Ionomycin (0.1–10 μM, 10 min) produced a concentration-dependent elevation in the amounts of both CaMKIIα and pCaMKIIα proteins bound to M4Rs (Figure 4D). This elevation was blocked by the CaMKII inhibitor KN93 (20 μM), which is able to inhibit the kinase by preventing the CaM binding (Figure 4E and F). The inactive analogue of KN93, KN92, had no effect. These results establish a Ca^{2+}-sensitive nature of CaMKIIα–M4R interactions in striatal neurons *in vivo*.

To directly confirm the accurate receptor site at which CaMKIIα binds, we developed an assay with Tat fusion peptides. We first synthesized an M4R interfering peptide (M4Ri) based on the core CaMKIIα-binding sequence on M4R$_{IL2}$ (YPARRTTKM). We assured that this peptide efficiently competed with M4R$_{IL2}$ for binding to CaMKIIα *in vitro* (Figure 4G). A sequence-scrambled control (MRRKPYATT, M4Rc), however, did not (Figure 4G). We then wanted to test the effect of these peptides in striatal neurons *in vivo*. To do so, we synthesized M4Ri or M4Rc together with an N-terminal Tat domain (YGRKKRRQRRR) derived from the human immunodeficiency virus-type 1 (HIV-1). This arginine-enriched Tat domain renders Tat fusion peptides a cell permeability in living neurons (Aarts *et al*, 2002; Liu *et al*, 2009). Using these cell-permeable peptides, we observed that Tat–M4Ri (2 μM, 45 min before ionomycin treatment) blocked the ionomycin-stimulated interactions between CaMKIIα and M4Rs in rat striatal slices, whereas Tat–M4Rc did not (Figure 4H). This indicates that Ca^{2+} rises in response to ionomycin can directly recruit CaMKIIα to an M4Ri-sensitive site on M4R$_{IL2}$. Moreover, ionomycin increased threonine phosphorylation of M4Rs, as detected by an antibody selective for phosphothreonine (Figure 4I).

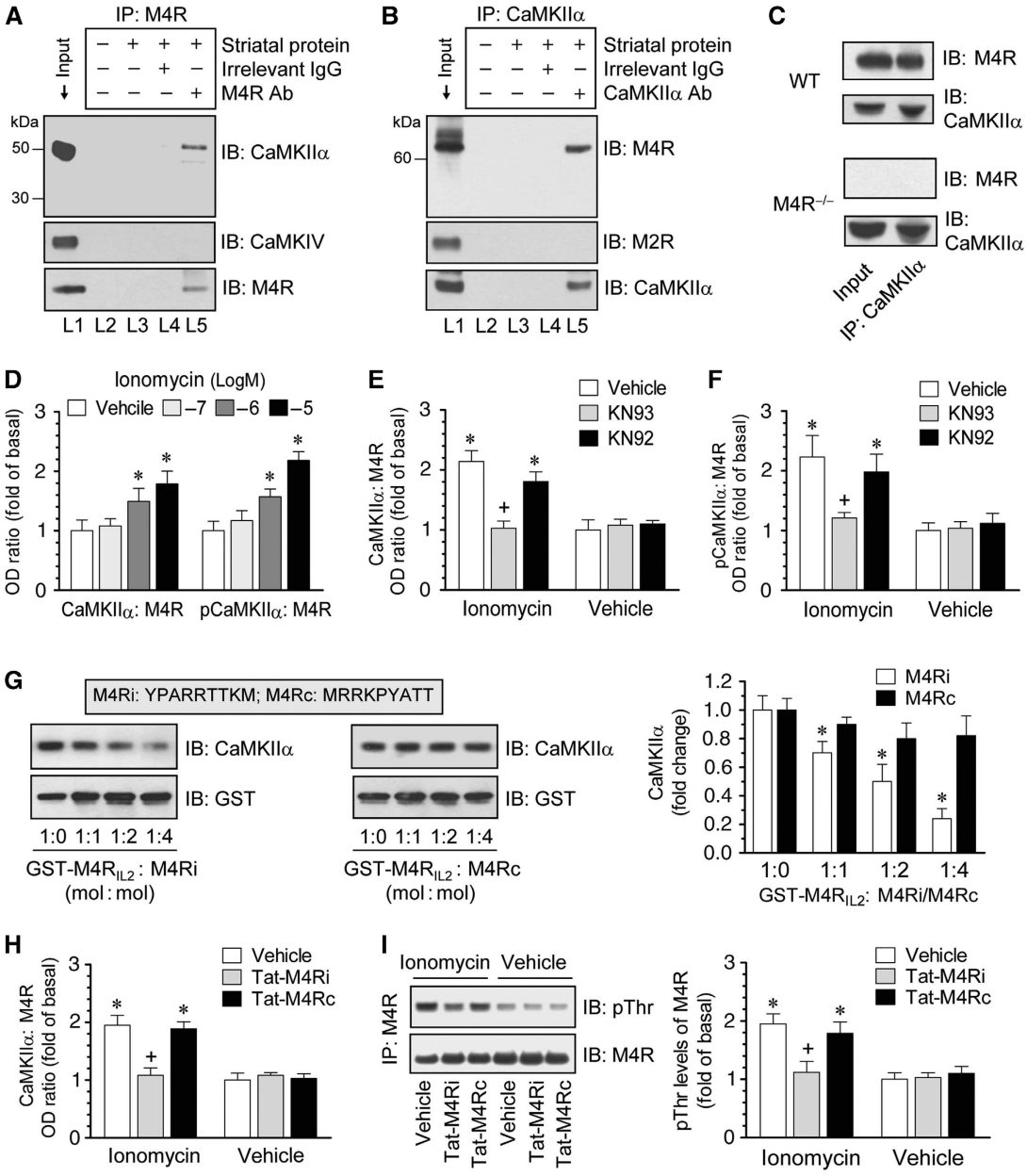

Figure 4 Interactions of CaMKIIα with M4Rs in striatal neurons. (**A**, **B**) Co-immunoprecipitation (IP) of CaMKIIα and M4Rs in the rat striatum. Lanes 3 and 4 showed no specific bands due to the lack of any antibody (L3) and the use of an irrelevant IgG (L4). (**C**) Co-immunoprecipitation of CaMKIIα and M4Rs in the striatum of wild-type (WT) and M4R mutant mice. (**D**) Effects of ionomycin (10 min) on the association of CaMKIIα and pCaMKIIα(T286) with M4Rs. (**E**, **F**) Effects of KN93 and KN92 on the ionomycin-stimulated association of CaMKIIα and pCaMKIIα(T286) with M4Rs. Ionomycin (10 μM) was co-treated with KN93 or KN92 (20 μM) for 10 min. (**G**) M4Ri disrupted the binding between CaMKIIα and $M4R_{IL2}$ *in vitro*. Bound CaMKIIα was visualized by immunoblots (IB). (**H**) Effects of Tat peptides on the ionomycin-induced association of CaMKIIα with M4Rs. (**I**) Effects of Tat peptides on the ionomycin-stimulated threonine phosphorylation of M4Rs. Tat peptides (2 μM) were applied 45 min before ionomycin treatment(10 μM, 10 min). Immunoblots of CaMKIIα, pCaMKIIα(T286), phosphothreonine (pThr), or M4Rs were performed on M4R precipitates from drug-treated striatal slices (**D**–**F**, **H**, **I**). The ratio of the optical density (OD) of CaMKIIα, pCaMKIIα, and pThr bands over M4R bands was calculated. Data are presented as means ± s.e.m. for 4–5 experiments per group. $^{*}P<0.05$ versus vehicle or vehicle + vehicle. $^{+}P<0.05$ versus vehicle + ionomycin.

This was blocked by pretreatment with Tat–M4Ri, but not Tat–M4Rc (Figure 4I). Thus, the inducible CaMKIIα interaction with $M4R_{IL2}$ constitutes an initial required step leading to the phosphorylation of the receptor. The selectivity of Tat–M4Ri in disrupting the CaMKIIα–M4R interaction was confirmed by the ineffectiveness of this peptide in interfering with the ionomycin-stimulated interaction between CaMKIIα and another substrate, NR2B (Gardoni *et al*, 1998; Leonard *et al*, 1999; Bayer *et al*, 2001; Supplementary Figure S5A). This selectivity is further supported by the finding that CaMKIIα I205K, an NR2B binding-defective mutant, could sufficiently bind to $M4R_{IL2}$ (Supplementary Figure S5B).

CaMKII potentiates M4R signalling

The next important question was what functional roles this Ca^{2+}-regulated interaction might have. We therefore investigated whether the CaMKII–M4R interaction regulates the M4R-coupled signalling pathway. The activation of Gαi/o-coupled M4Rs has been well documented to principally inhibit adenylyl cyclase, thereby lowering the rate of cAMP

production (Wess, 1996; Nathanson, 2000). We thus measured changes in cAMP levels as the signalling efficacy of M4Rs. In rat striatal slices, pharmacological activation of adenylyl cyclase with the selective activator, forskolin (1 or 10 μM, 10 min), substantially elevated the basal levels of cAMP (Supplementary Figure S6). The co-application of the mAChR-selective agonist, oxotremorine-M (10 μM), significantly reduced the forskolin-stimulated cAMP accumulation (Figure 5A), establishing a prevalent inhibition of the cAMP response by mAChRs in striatal neurons. Remarkably, co-adding ionomycin augmented the inhibition of cAMP responses in a concentration-dependent manner (Figure 5A). Oxotremorine-M or ionomycin alone did not alter basal cAMP levels (Figure 5B). Nor did ionomycin affect the forskolin-stimulated cAMP response (Figure 5C). These data demonstrate a Ca^{2+}-dependent potentiation of the inhibitory mAChR linkage to cAMP. The role of CaMKII in this linkage was supported by the following data. KN93 but not KN92 (20 μM) blocked the effect of ionomycin (Figure 5A). Tat–CaMKIINtide, a highly selective and cell-permeable inhibitory peptide of CaMKII (Chang *et al*, 1998; Vest *et al*, 2007), produced the same blocking effect when applied at 2 but not 0.2 μM (Figure 5D). To directly determine whether CaMKII acts through its interactions with M4Rs, we evaluated the importance of the CaMKII–M4R association. We observed that the CaMKII–M4R association interfering peptide Tat–M4Ri (2 but not 0.2 μM, 45 min before ionomycin/oxotremorine-M treatment) reversed the effect of ionomycin, whereas Tat–M4Rc did not (Figure 5E). Neither Tat–M4Ri nor Tat–M4Rc significantly altered the forskolin-stimulated cAMP formation or the oxotremorine-M-induced inhibition of cAMP responses to forskolin (data not shown). Thus, Ca^{2+}-activated CaMKII associates with M4Rs, thereby potentiating M4R efficacy in suppressing cAMP production.

Oxotremorine-M mainly stimulates M4Rs to inhibit cAMP responses. This is supported by experiments with the muscarinic toxin (MT). These MTs are small proteins from snake venoms, which display exquisite discrimination

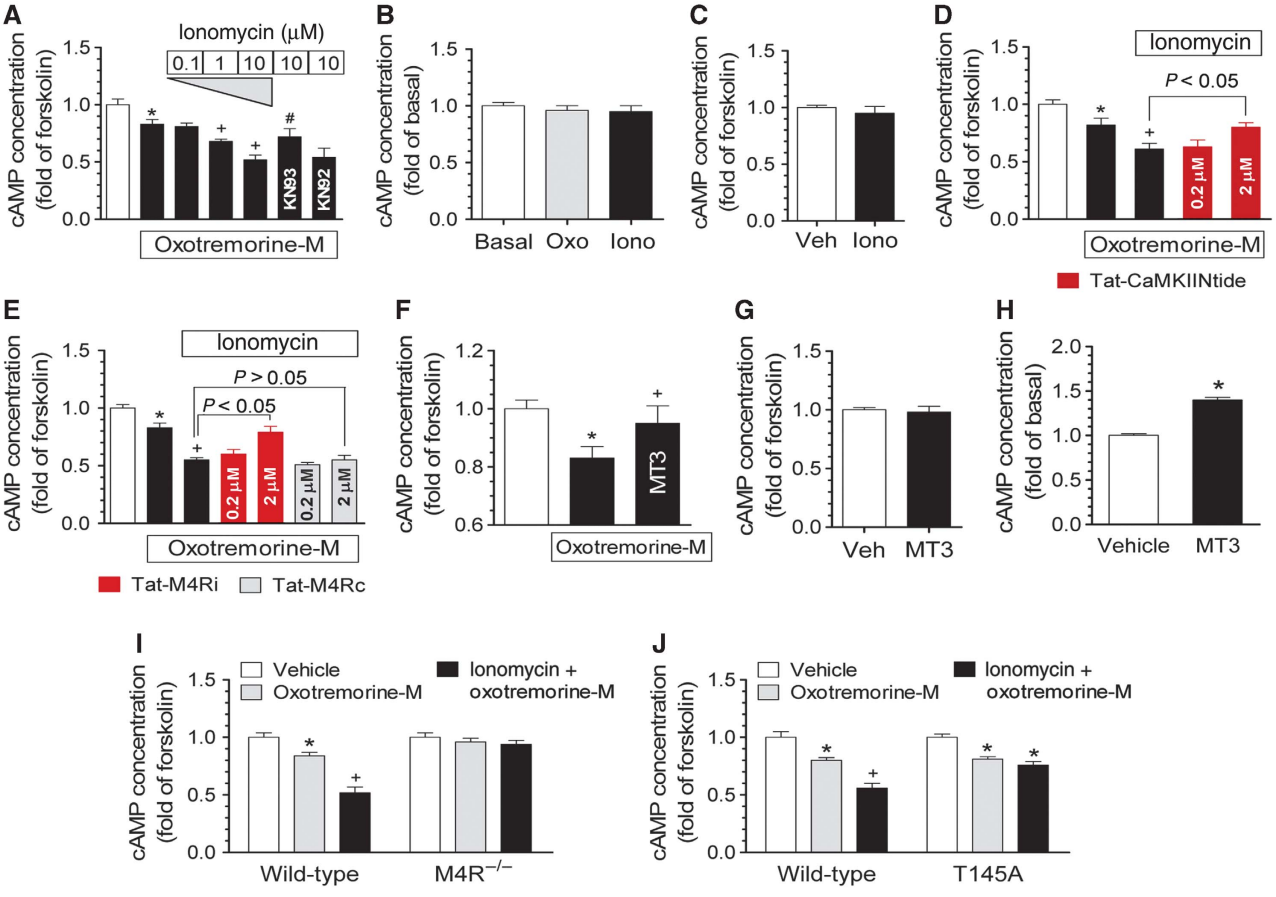

Figure 5 Regulation of M4R signalling by CaMKII. (**A**) Ionomycin potentiated the oxotremorine-M-induced inhibition of the forskolin-stimulated cAMP accumulation. (**B**) Oxotremorine-M (Oxo) or ionomycin (Iono) at 10 μM (10 min) did not alter basal cAMP levels. (**C**) Ionomycin (10 μM, 10 min) had no effect on the forskolin-stimulated cAMP formation. (**D**) Tat–CaMKIINtide reversed the effect of ionomycin. (**E**) Tat–M4Ri but not Tat–M4Rc blocked the effect of ionomycin. (**F**) MT3 blocked the oxotremorine-M-induced inhibition of the forskolin-stimulated cAMP accumulation. (**G**) MT3 did not alter the effect of forskolin. (**H**) Effects of MT3 (0.5 μM, 30 min) on basal cAMP concentrations. (**I**) Effects of oxotremorine-M on the forskolin-stimulated cAMP accumulation in wild-type (WT) and M4R mutant mice. (**J**) Ionomycin augmented the effect of oxotremorine-M in HEK293 cells transfected with WT M4Rs but not T145A mutants. Experiments were conducted on striatal slices from rats (**A**–**H**) or mice (**I**) or on HEK293 cells (**J**). Oxotremorine-M (10 μM), ionomycin (10 μM with 1 mM $CaCl_2$), KN93 (20 μM), and/or KN92 (20 μM) were co-incubated with forskolin (10 μM, 10 min) in (**A**, **C**, **I**, **J**). The Tat fusion peptide (Tat–CaMKIINtide, Tat–M4Ri, or Tat–M4Rc) was used at 0.2 or 2 μM 45 min before 10-min co-incubation of forskolin (10 μM) with oxotremorine-M (10 μM) and/or ionomycin (10 μM) in (**D**, **E**). MT3 (0.5 μM) was added 30 min before oxotremorine-M and/or forskolin (10 μM, 10 min) in (**F**, **G**). Data are presented as means ± s.e.m. for 4–7 experiments per group. $^{*}P<0.05$ versus forskolin alone (**A**, **D**, **E**, **F**, **I**, **J**) or vehicle (**H**). $^{+}P<0.05$ versus oxotremorine-M + forskolin (**A**, **D**, **E**, **F**, **I**, **J**). $^{\#}P<0.05$ versus ionomycin (10 μM).

among mAChR subtypes. Among MTs, MT3 is the most selective antagonist available for M4Rs. In fact, it has a 40-fold selectivity for the M4 over the M1 subtype and a greater than 500-fold selectivity for the M4 over the M2, M3, and M5 subtypes (Jolkkonen *et al*, 1994; Servent and Fruchart-Gaillard, 2009). Applying MT3 (0.5 μM) in rat striatal slices reversed the effect of oxotremorine-M in inhibiting cAMP responses to forskolin (Figure 5F). The protein, MT3, itself did not change forskolin-stimulated cAMP responses (Figure 5G). In addition, MT3 seemed to increase basal levels of cAMP (Figure 5H), indicating a tonic M4R activity in inhibiting basal cAMP formation. Consistent with the pharmacological blockade of M4Rs with MT3, genetic knockout of M4Rs prevented the oxotremorine-M effect. In striatal slices from M4R mutant mice, oxotremorine-M did not inhibit the forskolin-stimulated cAMP responses, whereas it did in WT mice (Figure 5I). In a mutagenesis study, the WT M4R or site-directed M4R mutant (T145A) was co-transfected with CaMKIIα in HEK293 cells. Ionomycin was found to potentiate the oxotremorine-M-induced suppression of cAMP responses to forskolin in cells transfected with WT M4Rs but not T145A mutants (Figure 5J).

The M4 receptors are predominant in striatonigral projection neurons that co-express dopamine D1 receptors (D1Rs; Ince *et al*, 1997; Santiago and Potter, 2001). We next explored the regulatory role of CaMKII–M4R interactions in D1-cAMP signalling. Adding the D1R agonist, SKF81297, in rat striatal slices enhanced cAMP accumulation in a concentration-dependent manner (Figure 6A). Co-adding the D1R antagonist, SCH23390, (10 μM) completely blocked this increase, confirming it as a D1R-mediated event (Figure 6B). Noticeably, similar to the observations with forskolin, the SKF81297-stimulated cAMP formation was attenuated by oxotremorine-M (Figure 6C). Co-applying ionomycin with oxotremorine-M induced a greater attenuation, which was blocked by KN93 but not KN92 (Figure 6C). Pretreatment with Tat–M4Ri rather than Tat–M4Rc also reversed the effect of ionomycin (Figure 6D). These data underscore an essential role of Ca^{2+}-dependent CaMKII–M4R interactions in regulating D1 signalling in striatal neurons and thus the acetylcholine–dopamine balance in the basal ganglia.

CaMKII–M4R$_{IL2}$ interactions regulate the striatal acetylcholine–dopamine balance in controlling behavioural activity

The proper integration of the two key transmitter systems (muscarinic cholinergic and dopaminergic neurotransmission) in the striatum coordinates motor activity (Di Chiara *et al*, 1994; Hauber, 1998). While D1Rs increase cAMP levels and motor activity, M4Rs inhibit them (Gomeza *et al*, 1999; Onali and Olianas, 2002; Tzavara *et al*, 2004; Sanchez-Lemus and Arias-Montano, 2006). Largely co-expressed D1Rs and M4Rs in striatonigral output neurons (Ince *et al*, 1997; Santiago and Potter, 2001) closely crosstalk to control the acetylcholine–dopamine balance and the dynamics of movement. In this study, we extended our above molecular studies to behavioural experiments to clarify whether regulated CaMKIIα–M4R interactions modify behavioural sensitivity to dopamine. The psychostimulant, cocaine, is known to increase extracellular dopamine and acetylcholine levels in the striatum (Church *et al*, 1987; Hurd and Ungerstedt, 1989; Imperato *et al*, 1993; Zocchi and Pert, 1994). This provides an *in vivo* model to evaluate the acetylcholine–dopamine balance and behaviours. A single intraperitoneal (i.p.) injection of cocaine (20 mg/kg) increased rat locomotor activity as determined in open-field assays (Figure 7A). Interestingly, pretreatment with an intravenous (i.v.) injection of the interfering Tat–M4Ri peptide (2 nmol/g, 45 min before cocaine

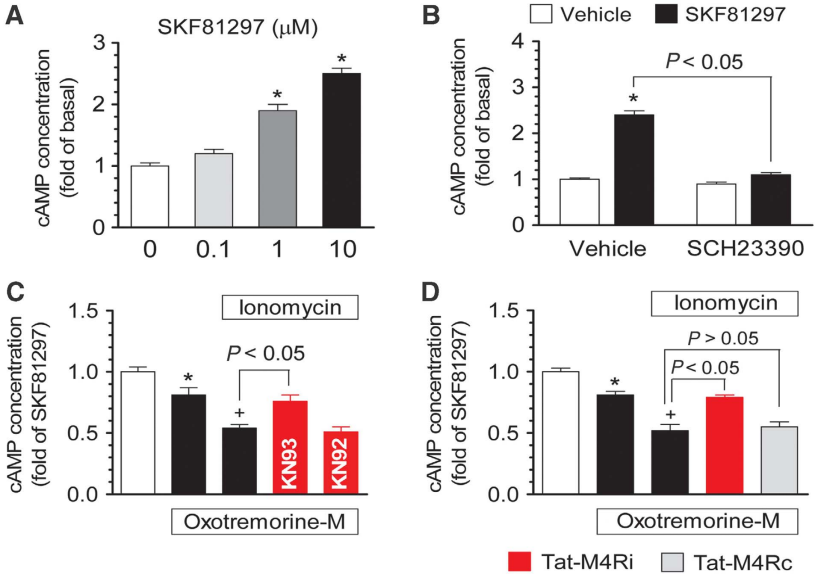

Figure 6 CaMKII potentiates the M4R-mediated inhibition of D1R–cAMP pathways in striatal neurons. (**A**) D1R stimulation with SKF81297 (0.1, 1, or 10 μM; 10 min) increased basal cAMP concentrations. (**B**) The D1R antagonist SCH23390 blocked the effect of SKF81297. SCH23390 (10 μM) was applied 10 min before SKF81297 (10 μM, 10 min). (**C**) Ionomycin augmented the inhibitory effect of oxotremorine-M on the SKF81297-stimulated cAMP formation. Oxotremorine-M (10 μM), ionomycin (10 μM with 1 mM $CaCl_2$), KN93 (20 μM), and/or KN92 (20 μM) were co-incubated with SKF81297 (10 μM, 10 min). (**D**) Tat–M4Ri, but not Tat–M4Rc, blocked the effect of ionomycin. Tat–M4Ri or Tat–M4Rc (2 μM) was added 45 min before 10-min co-incubation of SKF81297 (10 μM), oxotremorine-M (10 μM), and ionomycin (10 μM). Experiments were performed on rat striatal slices. Data are presented as means ± s.e.m. for 4–6 experiments per group. *$P<0.05$ versus basal levels (**A**, **B**) or SKF81297 alone (**C**, **D**). $^{+}P<0.05$ versus oxotremorine-M + SKF81297.

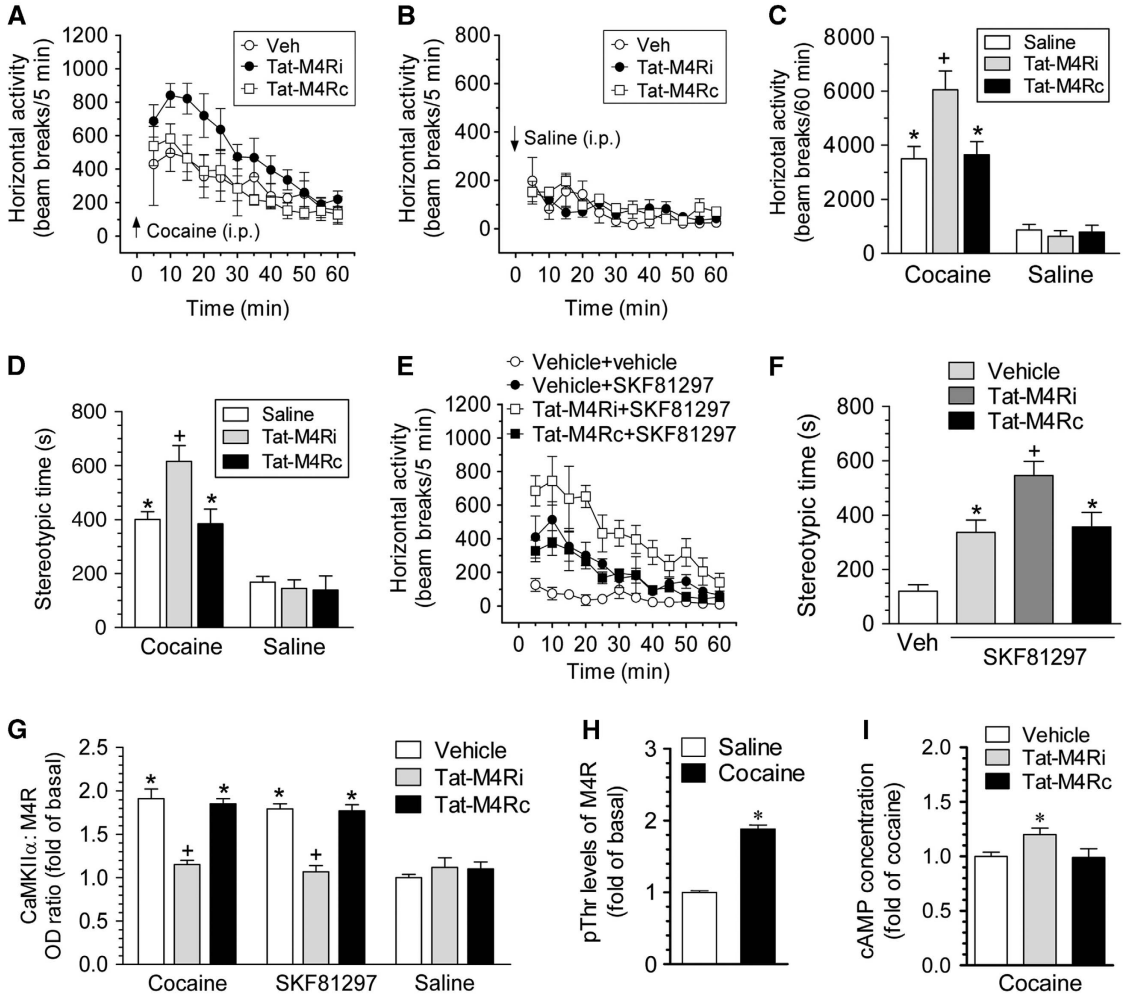

Figure 7 CaMKIIα–M4R interactions reduce motor responses to dopamine stimulation in rats. (**A**) Tat–M4Ri augmented locomotor responses to cocaine. (**B**) Tat–M4Ri had no effect on spontaneous motor activity. (**C**) A graph of the data from (**A**, **B**) obtained during 60 min after i.p. injection of drugs. (**D**) Tat–M4Ri augmented stereotypic responses to cocaine. (**E**) Tat–M4Ri augmented locomotor responses to SKF81297. (**F**) Tat–M4Ri augmented stereotypic responses to SKF81297. (**G**) Effects of Tat fusion peptides on basal and cocaine- or SKF81297-stimulated CaMKIIα–M4R interactions. (**H**) Cocaine increased threonine phosphorylation of M4Rs. (**I**) Tat–M4Ri augmented cAMP responses to cocaine. Cocaine (20 mg/kg, i.p.) or SKF81297 (2 mg/kg, i.p.) was injected alone or 45 min after an i.v. injection of Tat peptides at 2 nmol/g. Rats were killed 20 min after cocaine or SKF81297 injection for co-immunoprecipitation assays with striatal synaptosomal fractions and the M4R antibody (**G**, **H**) or for cAMP measurements with striatal tissue (**I**). Immunoblots of CaMKIIα, M4Rs, or phosphothreonine (pThr) were performed on M4R precipitates with the respective antibody. Data are presented as means ± s.e.m. ($n = 4$–10 per group). $^{*}P < 0.05$ versus saline + saline (**C**, **D**), vehicle (Veh) (**F**), vehicle + saline (**G**), saline (**H**), or vehicle + cocaine (**I**). $^{+}P < 0.05$ versus saline or vehicle + cocaine or SKF81297.

treatment) augmented locomotor responses to cocaine (Figure 7A). The control Tat–M4Rc peptide at the same dose had no effect (Figure 7A). Neither peptide alone altered spontaneous locomotor activity (Figure 7B and C). Similar results were observed in stereotypic activity surveyed by stereotypic time (Figure 7D). Tat–M4Ri, but not Tat–M4Rc (2 nmol/g), also enhanced locomotor and stereotypic responses to the D1 agonist SKF81297 (2 mg/kg, i.p.; Figure 7E and F). These data suggest that cocaine, while it activates D1Rs to stimulate motor activity, mobilizes the intrinsic CaMKII–M4R interaction to set a limitation on the motor response to cocaine. The disruption of this interaction lifts the limitation, resulting in a greater motor response to cocaine. In support of this, cocaine markedly increased the formation of CaMKIIα–M4R complexes in the rat striatum as detected by co-immunoprecipitation, and so did SKF81297 (Figure 7G). These increases were attenuated by Tat–M4Ri but not Tat-M4Rc (Figure 7G). Cocaine also increased threonine phosphorylation of striatal M4Rs (Figure 7H). In the presence of Tat–M4Ri, cocaine induced a greater increase in cAMP levels in striatal neurons (Figure 7I). The systemically active nature of short Tat fusion peptides of this kind has been well characterized in our previous work (Liu *et al*, 2006, 2009). In this study, using fluorescently tagged peptides (FITC–Tat–M4Ri), we observed a robust intracellular uptake of the peptide in striatal neurons 45–60 min after an i.v. injection at 2 nmol/g (data not shown).

Further behavioural experiments were performed in $M4R^{-/-}$ mice to substantiate the linkage of CaMKIIα–M4R interactions to movement. In wild-type mice, similar to rats in the above experiments, the disruption of CaMKIIα–M4R association with Tat–M4Ri (8 nmol/g, i.p., 60 min before cocaine treatment) enhanced locomotor responses to cocaine (Figure 8A). Tat–M4Rc did not alter the cocaine-stimulated hyperlocomotion (Figure 8A). In mutant mice, the stimulatory effect of cocaine was augmented, as evidenced by a 77% increase ($P < 0.05$) in locomotor responses to cocaine in mutant mice relative to wild-type mice. Unlike wild-type mice, no further augmentation of

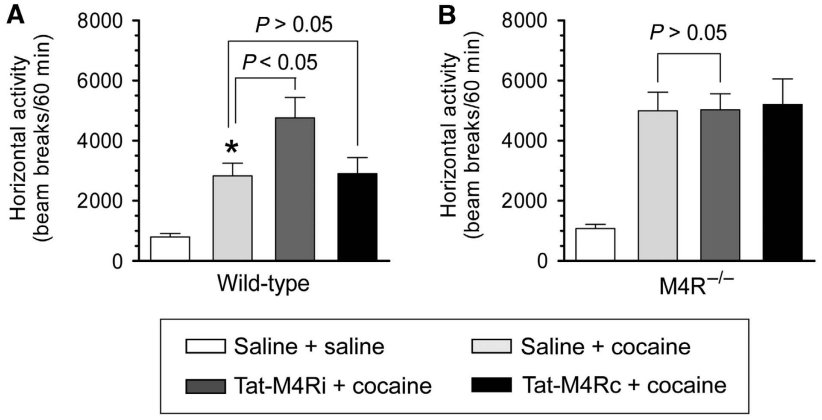

Figure 8 Effects of Tat fusion peptides on motor responses to cocaine in wild-type and $M4R^{-/-}$ mice. (**A**) Tat–M4Ri augmented locomotor responses to cocaine in wild-type mice. (**B**) Tat-M4Ri did not alter the cocaine-stimulated hyperlocomotion in $M4R^{-/-}$ mice. Cocaine (20 mg/kg, i.p.) was injected 60 min after a Tat peptide injection (8 nmol/g, i.p.). Data are presented as means ± s.e.m. ($n = 4$–8 per group). *$P < 0.05$ versus saline + saline.

locomotor responses to cocaine was observed in mutant mice pretreated with Tat–M4Ri (Figure 8B). These data support the role of CaMKIIα–M4R interactions in enhancing the M4R-mediated inhibition of motor sensitivity to cocaine.

Discussion

We investigated the interaction between CaMKII and M4Rs and roles of the interaction in regulating receptor function and behaviour in this study. We observed that CaMKIIα bound directly to the second cytoplasmic loop of M4Rs, whereas CaMKIIα did not bind to the same region of any other muscarinic receptor subtypes. The efficient binding occurred only after the activation of the enzyme by Ca^{2+}/CaM. The autophosphorylation of CaMKIIα further enhanced the binding affinity. Autophosphorylated CaMKIIα also binds to M4Rs in the absence of Ca^{2+}, indicating that the kinase, once activated and autophosphorylated, can sustain its binding even after transient Ca^{2+} rises subside (Meyer *et al*, 1992). The direct association of CaMKIIα implies M4Rs to be a biochemical substrate of the enzyme. Indeed, CaMKIIα phosphorylates $M4R_{IL2}$ at a specific threonine site. In rat striatal neurons expressing a high level of M4Rs, CaMKIIα was recruited to M4Rs by increasing Ca^{2+} level and thereby augmented receptor function. Behaviourally, the CaMKIIα–M4R interaction controls behavioural sensitivity to dopamine. Our data identify a new interaction linking Ca^{2+} to M4R physiology via CaMKIIα.

The finding that only the M4R among five muscarinic receptor subtypes harbours CaMKIIα is noteworthy. The defined binding site in the C-terminal region of $M4R_{IL2}$ contains R*XX*T residues, a sequence consistent with the consensus substrate recognition motif (R*XX*T/S) for CaMKII (White *et al*, 1998). Other three Gαq protein-coupled muscarinic receptor subtypes (M1, M3, and M5) also contain the R*XX*S motifs at different regions of the second intracellular loops (Supplementary Figure S2C). However, they failed to show detectable binding to CaMKIIα, indicating an insufficient nature of these motifs in the affinity for the kinase. $M2R_{IL2}$ shares a conserved sequence with $M4R_{IL2}$, but noticeably lacks a R*XX*T motif. Instead, it possesses a K*XX*T motif at the same site. This together with a difference in another residue may limit the affinity of $M2R_{IL2}$ for CaMKIIα, regardless of the fact that KXXT could also be a phosphorylation motif for the kinase. Another important characteristic of the CaMKIIα–M4R interaction is its Ca^{2+} dependency. Reliable binding between the two interacting partners requires preactivation of the enzyme by Ca^{2+} and CaM. Apparently, the CaMKIIα–$M4R_{IL2}$ interaction represents a regulatory mechanism that primarily operates in an activity-dependent manner, similar to another Ca^{2+}-activated interaction between CaM and third loops of M1, M2, and M3 receptors (Zhang *et al*, 2005; Lucas *et al*, 2006).

Striatal neurons express the highest level of M4Rs in the brain (Levey *et al*, 1991; Yasuda *et al*, 1993; Hersch *et al*, 1994). These Gαi/o-coupled M4Rs show a negative linkage to cAMP. Notably, this linkage was modulated by CaMKII in a synergistic manner. On the basis of our findings from neurochemical and signalling experiments, active CaMKII selectively binds to a defined intracellular site of M4Rs. This causes the phosphorylation of M4Rs at T145 and potentiates the M4R efficacy in inhibiting adenylyl cyclase. Given the fact that M4Rs are predominant in D1R-bearing striatonigral projection neurons as opposed to M1Rs in most striatal neurons and M2Rs in cholinergic interneurons (Yasuda *et al*, 1993; Hersch *et al*, 1994; Ince *et al*, 1997; Bernard *et al*, 1998; Alcantara *et al*, 2001; Santiago and Potter, 2001), the CaMKII–M4R synergy is likely to have a selective impact on D1 signalling. Indeed, disrupting the CaMKII–M4R association with Tat–M4Ri reduced the CaMKII/M4R-mediated inhibition of cAMP responses to a D1R agonist, confirming the role of CaMKII–M4R interactions in balancing D1 efficacy. The state-dependent nature of CaMKII–M4R interactions is another characteristic. Under basal conditions, CaMKII modulates M4Rs at a low level, corresponding to a low interaction rate between the two partners. Under a stimulated state, an enhanced D1R tone increases cAMP formation. Meanwhile, increased interactions of extracellular ligand and intracellular CaMKII with M4Rs render a synergistic inhibition of the D1-cAMP pathway. This provides a Ca^{2+}/activity-dependent mechanism to prevent overstimulation of D1 signalling or to induce a heterologous desensitization of D1R responses. Interference with the CaMKII–M4R coupling by Tat–M4Ri could then reduce the M4R-mediated inhibition of the D1-cAMP pathway and allow greater cAMP responses to D1 stimulation.

Balanced D1R and M4R activity in striatonigral efferent neurons intimately controls the 'direct pathway' outflow and movement (Di Chiara *et al*, 1994; Hauber, 1998). In response to cocaine, synaptic dopamine in the striatum was elevated as

a result of blockade of the dopamine reuptake into nerve terminals (Church *et al*, 1987; Hurd and Ungerstedt, 1989). Elevated dopamine activates D1Rs on striatonigral neurons to increase cAMP levels and activate downstream protein kinase A, which thereby upregulates excitability of these neurons and stimulates motor activity (Surmeier *et al*, 2007). Similar to dopamine, local acetylcholine release was increased in response to cocaine (Imperato *et al*, 1993; Zocchi and Pert, 1994). This change is to balance the elevated dopaminergic tone in the basal ganglia. Through co-expressed M4Rs, acetylcholine limits D1 stimulation of striatonigral neurons and restricts motor responses to cocaine. Interestingly, the M4R function in balancing D1Rs requires a synergistic cooperation with CaMKII. As demonstrated in this study, dopamine stimulation using cocaine increased the CaMKII association with M4Rs in striatal neurons. A D1 agonist also increased the CaMKII–M4R association. In this case, the Ca^{2+} activation of CaMKII might result from the direct activation of Gαq-coupled D1Rs that release Ca^{2+} from intracellular stores through a phospholipase Cβ (PLCβ)-dependent mechanism (Felder *et al*, 1989; Undie and Friedman, 1990) or the indirect activation of Ca^{2+}-permeable glutamate receptors (Andre *et al*, 2010). The elevated association promotes M4Rs to suppress motor responses to cocaine, as the disruption of this interaction by an interfering peptide (Tat–M4Ri) weakened the efficacy of M4Rs in confining motor responses to cocaine. Together, M4Rs that are strategically localized in the basal ganglia for balancing dopaminergic transmission are actively regulated by a previously unrecognized mechanism. By modifying the interaction rate with M4Rs and phosphorylating the receptor at a distinct site, CaMKII dynamically regulates the acetylcholine–dopamine balance and maintains a proper homeostasis in the striatum.

Materials and methods

Animals

Adult male Wistar rats weighting 200–225 g (Charles River, New York, NY), adult WT mice, and mutant mice lacking M4Rs were individually housed at 23°C and 50 ± 10% humidity with food and water available *ad libitum*. The animal room was on a 12:12 h light/dark cycle with lights on at 0700 hours. All animal use procedures were in strict accordance with the NIH Guide for the Care and Use of Laboratory Animals and were approved by the Institutional Animal Care and Use Committee.

Cloning, expression, and purification of GST fusion proteins

The cDNA fragments encoding the $M4R_{IL2}$(D128-M147), $M4R_{IL3}$ (H216-K254), $M4R_{IL3}$(K255-A370), $M4R_{IL3}$(N371-T400), $M4R_{CT}$(N456-R478), $M1R_{IL2}$(D122-R141), $M2R_{IL2}$(D120-M139), $M3R_{IL2}$(D164-R183), $M5R_{IL2}$(D126-R145), $CaMKII\alpha_{CD}$(L91-S272), $CaMKII\alpha_{RD}$(H273-S314), or $CaMKII\alpha_{AD}$(G315-H478) were generated by PCR amplification from full-length cDNA clones. These fragments were subcloned into *Bam*HI–*Eco*RI sites of the pGEX4T-3 plasmid (Amersham Biosciences, Arlington Heights, IL). Initiation methionine residues and stop codons were also incorporated where appropriate. To confirm appropriate splice fusion, all constructs were sequenced. The GST fusion proteins were expressed in *Escherichia coli* BL21 cells (Amersham) and purified from bacterial lysates as described by the manufacturer. The GST- or His-tagged full-length CaMKIIα (M1-H478) and GST-tagged full-length CaMKIV (M1-Y473) were expressed and purified via a baculovirus/Sf9 insect cell expression system.

Affinity purification (pull-down) assay

Solubilized striatal extracts (50–100 μg of protein) were diluted with 1 × PBS/1% Triton X-100 and incubated with 50% (v/v) slurry of glutathione–Sepharose 4B beads (Amersham) saturated with GST alone or with the indicated GST fusion protein (5–10 μg) for 2–3 h at 4°C. Beads were washed four times with 1 × PBS/1% Triton X-100. Bound proteins were eluted with 2 × lithium dodecyl sulfate (LDS) sample buffer, resolved by SDS–PAGE, and immunoblotted with a specific antibody.

In vitro binding assay

His-tagged CaMKIIα WT (~57 kDa), WT pCaMKIIα, or CaMKIIα mutants (~50 kDa) were equilibrated to binding buffer (200 mM NaCl, 0.2% Triton X-100, 0.1 mg/ml BSA, and 50 mM Tris (pH 7.5)) with or without 0.5 mM $CaCl_2$, 1 μM CaM, 1 mM EGTA, or 50 μM ATP as indicated. Binding reactions were initiated by adding purified GST fusion proteins and were maintained at 4°C for 2–3 h unless otherwise indicated. The GST fusion proteins were precipitated using 100 μl of 10% glutathione–Sepharose. The precipitate was washed three times with binding buffer. Bound proteins were eluted with 2 × LDS loading buffer, resolved by SDS–PAGE, and immunoblotted with a specific antibody.

cAMP enzyme immunoassay

Striatal slices or striatal brain tissue were homogenized in 0.1 M HCl solution for 15 min with gentle shaking and spun in the microcentrifuge tubes. The concentrations of cAMP of the supernatant were measured using the Direct cAMP Enzyme Immunoassay (EIA) Kit (Assay Designs, Ann Arbor, MI) following the manufacturer's instruction. Protein concentrations were determined using a BCA Protein Assay kit (Pierce). The activity of M4Rs was determined by measuring inhibition of forskolin-stimulated cAMP formation because oxotremorine-M had a minimal effect on basal cAMP levels.

Behavioural assessments

Locomotion in an open field was evaluated as described previously (Liu *et al*, 2006; Mao *et al*, 2009). Stereotypic activities were recorded as stereotypic time, which refers to the total time that stereotypic behaviours (repetitive breaks of a given beam or beams with an interval less than 1 s) were observed.

Supplementary data

Supplementary data are available at *The EMBO Journal* Online (http://www.embojournal.org).

Acknowledgements

We thank Dr Jurgen Wess (NIDDK/NIH) for providing M4R knockout mice and age- and genetic background-matched (129SvEV/CF1) WT mice; Dr Howard Schulman, Dr K Ulrich Bayer, and Dr Yasunori Hayashi for providing CaMKIIα WT and mutant vectors; and Ms Lucy S Wang for technical support and comments. This study was supported by NIH grants DA10355 (JQW) and MH61469 (JQW), and by a grant from Saint Luke's Hospital Foundation.

Conflict of interest

The authors declare that they have no conflict of interest.

References

Aarts M, Liu Y, Liu L, Besshoh S, Arundine M, Gurd JW, Wang YT, Salter MW, Tymianski M (2002) Treatment of ischemic brain damage by perturbing NMDA receptor–PSD-95 protein interactions. *Science* **298:** 846–850

Alcantara AA, Mrzliak L, Jakab RL, Levey AI, Hersch SM, Goldman-Rakic PS (2001) Muscarinic m1 and m2 receptor proteins in local circuit and projection neurons of the primate striatum: anatomical evidence for cholinergic modulation of glutamatergic prefronto-striatal pathways. *J Comp Neurol* **434:** 445–460

Andre VM, Cepeda C, Cummings DM, Jocoy EL, Fisher YE, Yang WX, Levine MS (2010) Dopamine modulation of excitatory currents in the striatum is dictated by the expression of D1 or D2 receptors and modified by endocannabinoids. *Eur J Neurosci* **31:** 14–28

Bayer KU, Koninck PD, Leonard AS, Hell JW, Schulman H (2001) Interaction with the NMDA receptor locks CaMKII in an active conformation. *Nature* **411:** 801–805

Bernard V, Laribi O, Levey AI, Bloch B (1998) Subcellular redistribution of m2 muscarinic acetylcholine receptors in striatal interneurons *in vivo* after acute cholinergic stimulation. *J Neurosci* **18:** 10207–10218

Chang BH, Mukherji S, Soderling TR (1998) Characterization of a calmodulin kinase II inhibitor protein in brain. *Proc Natl Acad Sci USA* **95:** 10890–10895

Church WH, Justice Jr JB, Byrd LD (1987) Extracellular dopamine in rat striatum following uptake inhibition by cocaine, nomifensine and benztropine. *Eur J Pharmacol* **139:** 345–348

Colbran RJ (2004) Targeting of calcium/calmodulin-dependent protein kinase II. *Biochem J* **378:** 1–16

Colbran RJ, Brown AM (2004) Calcium/calmodulin-dependent protein kinase II and synaptic plasticity. *Curr Opin Neurobiol* **14:** 318–327

Colbran RJ, Soderling TR (1990) Calcium/calmodulin-independent autophosphorylation sites of calcium/calmodulin-dependent protein kinase II. Studies on the effect of phosphorylation of threonine 305/306 and serine 314 on calmodulin binding using synthetic peptides. *J Biol Chem* **265:** 11213–11219

Di Chiara G, Morelli M, Consolo S (1994) Modulatory functions of neurotransmitters in the striatum: Ach/dopamine/NMDA interactions. *Trends Neurosci* **17:** 228–233

Felder CC, Jose PA, Axelrod J (1989) The dopamine-1 agonist, SKF82526, stimulates phospholipase-C activity independent of adenylate cyclase. *J Pharmacol Exp Ther* **248:** 171–175

Gardoni F, Caputi A, Cimino M, Pastorino L, Cattabeni F, Di Luca M (1998) Calcium/calmodulin-dependent protein kinase II is associated with NR2A/B subunits of NMDA receptor in postsynaptic densities. *J Neurochem* **71:** 1733–1741

Gomeza J, Zhang L, Kostenis E, Felder C, Bymaster F, Brodkin J, Shannon H, Xia B, Deng CX, Wess J (1999) Enhancement of D1 dopamine receptor-mediated locomotor stimulation in M_4 muscarinic acetylcholine receptor knockout mice. *Proc Natl Acad Sci USA* **96:** 10483–10488

Griffith LC (2004) Regulation of calcium/calmodulin-dependent protein kinase II activation by intramolecular and intermolecular interactions. *J Neurosci* **24:** 8394–8398

Hauber W (1998) Involvement of basal ganglia transmitter systems in movement initiation. *Prog Neurobiol* **56:** 507–540

Hersch SM, Gutekunst CA, Rees HD, Heilman CJ, Levey AI (1994) Distribution of m1-m4 muscarinic receptor proteins in the rat striatum: light and electron microscopic immunocytochemistry using subtype-specific antibodies. *J Neurosci* **14:** 3351–3363

Hudmon A, Schulman H (2002) Neuronal Ca^{2+}/calmodulin-dependent protein kinase II: the role of structure and autoregulation in cellular function. *Annu Rev Biochem* **71:** 473–510

Hurd YL, Ungerstedt U (1989) Cocaine: an *in vivo* microdialysis evaluation of its acute action on dopamine transmission in rat striatum. *Synapse* **3:** 48–54

Imperato A, Obinu MC, Gessa GL (1993) Effects of cocaine and amphetamine on acetylcholine release in the hippocampus and caudate nucleus. *Eur J Pharmacol* **238:** 377–381

Ince E, Ciliax BJ, Levey AI (1997) Differential expression of D1 and D2 dopamine and m4 muscarinic acetylcholine receptor proteins in identified striatonigral neurons. *Synapse* **27:** 357–366

Jolkkonen M, Van Giersbergen PL, Hellman U, Wernstedt C, Karlsson E (1994) A toxin from the green mamba *Dendroaspis angusticeps*: amino acid sequence and selectivity for muscarinic m4 receptors. *FEBS Lett* **352:** 91–94

Kelly PT, McGuinness TL, Greengard P (1984) Evidence that the major postsynaptic density protein is a component of a Ca^{2+}/calmodulin-dependent protein kinase. *Proc Natl Acad Sci USA* **81:** 945–949

Langmead CJ, Watson J, Reavill C (2008) Muscarinic acetylcholine receptors as CNS drug targets. *Pharmacol Ther* **117:** 232–243

Leonard AS, Lim IA, Hemsworth DE, Horne MC, Hell JW (1999) Calcium/calmodulin-dependent protein kinase II is associated with the *N*-methyl-D-aspartate receptor. *Proc Natl Acad Sci USA* **96:** 3239–3244

Levey AL, Kitt CA, Simonda WF, Price DL, Brann MR (1991) Identification and localization of muscarinic acetylcholine receptor proteins in brain with subtype-specific antibodies. *J Neurosci* **11:** 3218–3226

Lisman J, Schlman H, Cline H (2002) The molecular basis of CaMKII function in synaptic and behavioral memory. *Nat Rev Neurosci* **3:** 175–190

Liu XY, Chu XP, Mao LM, Wang M, Lan HX, Li MH, Zhang GC, Parelkar NK, Fibuch EE, Haines M, Neve KA, Liu F, Xiong ZG, Wang JQ (2006) Modulation of D2R–NR2B interactions in response to cocaine. *Neuron* **52:** 897–909

Liu XY, Mao LM, Zhang GC, Papasian CJ, Fibuch EE, Lan HX, Zhou HF, Xu M, Wang JQ (2009) Activity-dependent modulation of limbic dopamine D3 receptors by CaMKII. *Neuron* **61:** 425–438

Lucas JL, Wang D, Sadee W (2006) Calmodulin binding to peptides derived from the i3 loop of muscarinic receptors. *Pharm Res* **23:** 647–653

Mao LM, Wang W, Chu XP, Zhang GC, Liu XY, Yang YJ, Haines M, Papasian CJ, Fibuch EE, Buch S, Chen JG, Wang JQ (2009) Stability of surface NMDA receptors controls synaptic and behavioral adaptations to amphetamine. *Nat Neurosci* **12:** 602–610

Meyer T, Hanson PI, Stryer L, Schulman H (1992) Calmodulin trapping by calcium–calmoduliFn-dependent protein kinase. *Science* **256:** 1199–1201

Nathanson NM (2000) A multiplicity of muscarinic mechanism: enough signaling pathways to take your breath away. *Proc Natl Acad Sci USA* **97:** 6245–6247

Nathanson NM (2008) Synthesis, trafficking, and localization of muscarinic acetylcholine receptors. *Pharmacol Ther* **119:** 33–43

Onali P, Olianas MC (2002) Muscarinic M_4 receptor inhibition of dopamine D1-like receptor signalling in rat nucleus accumbens. *Eur J Pharmacol* **448:** 105–111

Sanchez-Lemus E, Arias-Montano JA (2006) M_1 muscarinic receptors contribute to, whereas M_4 receptors inhibits, dopamine D1 receptor-induced [^{3}H]-cyclic AMP accumulation in rat striatal slices. *Neurochem Res* **31:** 555–561

Santiago MP, Potter LT (2001) Biotinylated m4-toxin demonstrate more M4 muscarinic receptor protein on direct than indirect striatal projection neurons. *Brain Res* **894:** 12–20

Scarr E, Dean B (2008) Muscarinic receptors: do they have a role in the pathology and treatment of schizophrenia? *J Neurochem* **107:** 1188–1195

Servent D, Fruchart-Gaillard C (2009) Muscarinic toxins: tools for the study of the pharmacological and functional properties of muscarinic receptors. *J Neurochem* **109:** 1193–1202

Surmeier DJ, Ding J, Day M, Wang Z, Shen W (2007) D1 and D2 dopamine-receptor modulation of striatal glutamatergic signaling in striatal medium spiny neurons. *TINS* **30:** 228–235

Tzavara ET, Bymaster FP, Davis RJ, Wade MR, Perry KW, Wess J, McKinzie DL, Felder C, Nomikos GG (2004) M_4 muscarinic receptors regulate the dynamics of cholinergic and dopaminergic neurotransmission: relevance to the pathophysiology and treatment of related central nervous system pathologies. *FASEB J* **18:** 1410–1412

Undie AS, Friedman E (1990) Stimulation of a dopamine D1 receptor enhances inositol phosphates formation in rat brain. *J Pharmacol Exp Ther* **253:** 987–992

Vest RS, Davies KD, O'Leary H, Prot JD, Bayer KU (2007) Dual mechanism of a natural CaMKII inhibitor. *Mol Biol Cell* **18:** 5024–5033

Wess J (1996) Molecular biology of muscarinic acetylcholine receptors. *Crit Rev Neurobiol* **10:** 69–99

White RR, Kwon YG, Taing M, Lawrence DS, Edelman AM (1998) Definition of optimal substrate recognition motifs of Ca^{2+}-calmodulin-dependent protein kinases IV and II reveals shared and distinctive features. *J Biol Chem* **273:** 3166–3179

Yasuda RP, Ciesla W, Flores LR, Wall SJ, Li M, Satkus SA, Weisstein JS, Spagnola BV, Wolfe BB (1993) Development of antisera selective for m4 and m5 muscarinic cholinergic receptors: distribution of m4 and m5 receptors in rat brain. *Mol Pharmacol* **43:** 149–157

Zhang Y, Wang D, Sadee W (2005) Calmodulin interaction with peptides from G-protein coupled receptors measured with S-Tag labeling. *Biochem Biophys Res Comm* **333:** 390–395

Zocchi A, Pert A (1994) Alterations in striatal acetylcholine overflow by cocaine, morphine, and MK-801: relationship to locomotor output. *Psychopharmacology (Berl)* **115:** 297–304